environments

Article

Magnetic Susceptibility as a Proxy for Metal Enrichment in Karstic Estuarine Sediments: A Case Study on the Krka River, Croatia

Stanislav Frančišković-Bilinski, Neven Cukrov and Nuša Cukrov *

Division for Marine and Environmental Research, Ruđer Bošković Institute, Bijenička Cesta 54, 10000 Zagreb, Croatia; francis@irb.hr (S.F.-B.); ncukrov@irb.hr (N.C.)
* Correspondence: cukrov@irb.hr

Abstract

To evaluate the use of the magnetic susceptibility (MS) method as a rapid screening tool for metal enrichment in the karst estuarine systems, a case study was conducted in the Krka River Estuary (Croatia). Magnetic measurements were performed on 36 surface sediment samples collected along the entire estuary, as well as in 6 sediment cores taken from areas with different sedimentological properties and/or varying levels of anthropogenic pressure. The efficacy of MS as a proxy for metal enrichment was evaluated by correlating the obtained datasets with previously published metal concentrations in the same samples, utilising statistical methods to quantify these relationships. Susceptibility values in the Krka River Estuary are generally low (mean value 0.123 × 10^{-3} SI), reflecting a carbonate-dominated background typical of uncontaminated karst systems, but various local anomalies (max value 0.799 × 10^{-3} SI) coincide with areas of metal enrichment previously linked to industrial and port activities. Correlation and multivariate analyses show that, despite a low overall magnetic signal, elevated MS can successfully detect hotspots with increased metal levels (e.g., Pb, Mn), confirming that with careful calibration to local magnetic background values, this method provides an effective and analytically simple proxy for metal-enriched sediments in sensitive karst estuaries.

Keywords: environmental magnetism; anthropogenic impact; sediment contamination; metals; Adriatic; karstic estuary

Academic Editor: Chihhao Fan

Received: 7 March 2026
Revised: 13 April 2026
Accepted: 23 April 2026
Published: 4 May 2026

1. Introduction

Magnetic susceptibility (MS) has become a widely used, rapid, and cost-effective method for assessing metal enrichment in soils and sediments. Because ferric and paramagnetic iron oxides often host, adsorb, or co-precipitate with potentially toxic metals, changes in MS can reflect spatial patterns and vertical distributions of elements such as Pb, Zn, Cu, Cd, Ni, and Cr in terrestrial and aquatic environments. The development and application of this method in environmental research began in the late 1980s and 1990s, pioneered by Thompson and Oldfield [1]. Subsequently, several authors have investigated the use of magnetic measurements as a substitute for chemical analyses in environmental surveys, which are expensive and complex [2–9]. Petrovský and Ellwood [10] provided a detailed overview of the use of magnetic methods in environmental research. These authors promoted the MS method as a "reliable, rapid, and cost-effective proxy for

identifying industrial heavy metal pollution in soils and sediments". They found that anthropogenic contamination with heavy metals often corresponds with the emission of ferrimagnetic particles, such as magnetite or maghemite, which are the main cause of increased magnetic susceptibility in the surrounding environment. They also showed a strong spatial correlation between elevated MS values and increased concentrations of heavy metals such as Pb, Zn, and Cu. This was successfully demonstrated in the case of the Litavka River (Czech Republic), where they found very similar distribution patterns between MS and Zn, caused by the presence of lead smelter ashes. The main advantage of the MS method is that it enables low-cost on-site detection of heavy metal hotspots, reducing the need for extensive chemical laboratory analysis. Most authors now agree that the MS method is a promising and reliable approach for identifying contaminated areas. Studies conducted in various aquatic environments, including estuarine [11–13], coastal [14–18], lacustrine [19,20], and fluvial [21–23] areas, show positive correlations between MS and metals such as Pb, Zn, Cu, Co, and Mn, demonstrating that MS-based screening can rapidly identify contaminated sites and vertical pollution history, especially when assisted by multivariate statistics or machine learning models. Due to its low cost and efficiency, it is possible to cover a dense network of sampling points and identify the most important locations where chemical analyses should also be conducted. However, the method has limitations, as the reliability of MS as an indicator of contamination is strongly influenced by the parent material, land use, and depositional processes. Where lithogenic magnetic minerals dominate, or where multiple metal sources separate metals from magnetic carriers, susceptibility may reflect natural geology rather than anthropogenic loading or show weak and scale-dependent relationships with pollutants [24]. For example, karst wetlands provide a case where enhanced magnetic signals mainly reflect pedogenic Fe oxides [25], while potentially toxic metals show only weak coupling to magnetic carriers, highlighting the need for site-specific calibration. In river systems, moreover, sediment may originate from long-distance transport and undergo various transformations along the way, which can significantly alter the original elemental composition of particles and weaken the relationship between magnetic minerals and potentially toxic metals. Metals can be structurally incorporated into magnetic minerals during combustion in industrial processes or adsorbed onto the surface of magnetic mineral nanoparticles, as typically observed for Zn and Pb. As these latter bonds are relatively weak, fluvial transport can facilitate the separation of metals from their magnetic carriers, ultimately weakening the statistical correlation between MS and metal concentrations and thus reducing the efficacy of MS as a proxy for environmental metal enrichment [26]. These contrasting findings underscore the importance of understanding the controls on magnetic mineralogy and calibrating susceptibility to metal concentrations before using it as an indicator of metal enrichment.

In recent years, MS research has intensified across various environments and with different objectives. Numerous authors have investigated the following processes using magnetic methods: environmental profile assessment of a highly industrialised area [27]; rapid characterisation of coastal morphosedimentary units [28]; palaeoenvironmental investigations based on magnetic mineral dissolution in lacustrine sediment cores [29]; provenance studies of marine sediments [30]; investigations of acid-mine drainage contamination in sediments [31]; environmental indications of grain size and MS in Quaternary sediments from tidal channels [32]; and investigation of coarse- and fine-grained sediment magnetic properties along the entire course of a river [33], among others.

Despite many coastal and estuarine applications of the MS method as a proxy for metal enrichment, there is currently limited knowledge regarding karst estuarine systems. Most existing work focuses on the siliciclastic or volcanic settings, leaving the research gap regarding the efficiency of MS as a metal screening tool in areas where carbonate

lithology controls the background magnetic signals. To explore the potential and limitations of this method in karst environments, this study focused on the Krka River Estuary, a karstic river partially affected by potentially toxic metals. The site offers an ideal opportunity to study the interaction of karst lithology, estuarine hydrodynamics, and the mixed natural and anthropogenic origins of the studied elements and acts as an ideal natural laboratory to study their connections with MS. The Krka River Estuary stands as the most prominent karst estuary on the eastern Adriatic coast. Due to its distinctive nature, it has become the most extensively studied estuary in the region, with numerous papers published describing various biogeochemical and physical aspects of the estuarine environment [34–43]. While a previous study on Lake Prokljan (part of the Krka River Estuary) utilised MS [44], its research focus was not directed towards the determination of metal enrichment in the sediment and assessment of the contamination levels. To our knowledge, this is the first application of the MS method specifically as a proxy of metal enrichment in estuarine and marine sediments in Croatia. Until now, it has only been used in such a capacity for the investigation of river sediments [45,46] and soils [47]. Accordingly, the present study addresses three primary objectives: (i) to quantify the spatial and vertical distribution of MS in karst estuarine sediments under mixed natural and anthropogenic influence; (ii) to evaluate the relationship between MS and potentially toxic metals under the control of carbonate lithology, using previously reported elemental concentrations and multivariate statistics; and (iii) to identify specific conditions and limitations under which MS can serve as a reliable, low-cost proxy for screening metal enrichment in karstic aquatic environments. We hope that current research will contribute to the global promotion of the MS method in environmental research and enhance overall knowledge of environmental magnetism.

2. Materials and Methods

2.1. Study Area

The Krka River Estuary is a 22 km long, microtidal karst system located on the eastern Adriatic coast (Figure 1). Due to the low tidal range (0.2–0.5 m) and its sheltered position, the estuary remains permanently stratified, with a freshwater surface layer and a landward-moving salt wedge. The Krka River itself delivers very little suspended material (<6 mg L^{-1}) [37] because of the upstream tufa barriers, which act as natural sediment transport barriers. Most terrigenous material instead enters the system via the Guduča River, a small tributary that drains flysch deposits and flows into the upper part of the estuary (Prokljan Lake) [48,49]. Sedimentation patterns vary significantly along the estuary. In the upper part, the sediment consists of a mixture of terrigenous material and carbonates, with sedimentation rates between 2 and 5 mm $year^{-1}$ (higher sedimentation rate closer to the Guduča River) [50] and finer grain sizes. In contrast, the lower part (Šibenik Bay) is dominated by marine biogenic carbonates [49], with much slower sedimentation rates (<1 mm $year^{-1}$) [50] and coarser grains. The upper and lower estuary also differ in terms of anthropogenic impact. While the upper reaches remain relatively pristine, the lower estuary has been affected by the industrial activities of the city of Šibenik [41,43,51,52]. Historical pollution sources include a ferroalloy (Fe-Mn) factory (TEF) that operated until the mid-1990s, a phosphate transhipment port, and a repair shipyard. Although industrial production has ceased and port and shipyard facilities have been modernised, elevated concentrations of metals such as Mn, Pb, Zn, Cu, and Hg are still present in the surface sediments [52]. Due to the presence of various sources of anthropogenic pressure in Šibenik Bay, the estuary is a particularly interesting area for testing MS as a convenient assessment tool for metal loading.

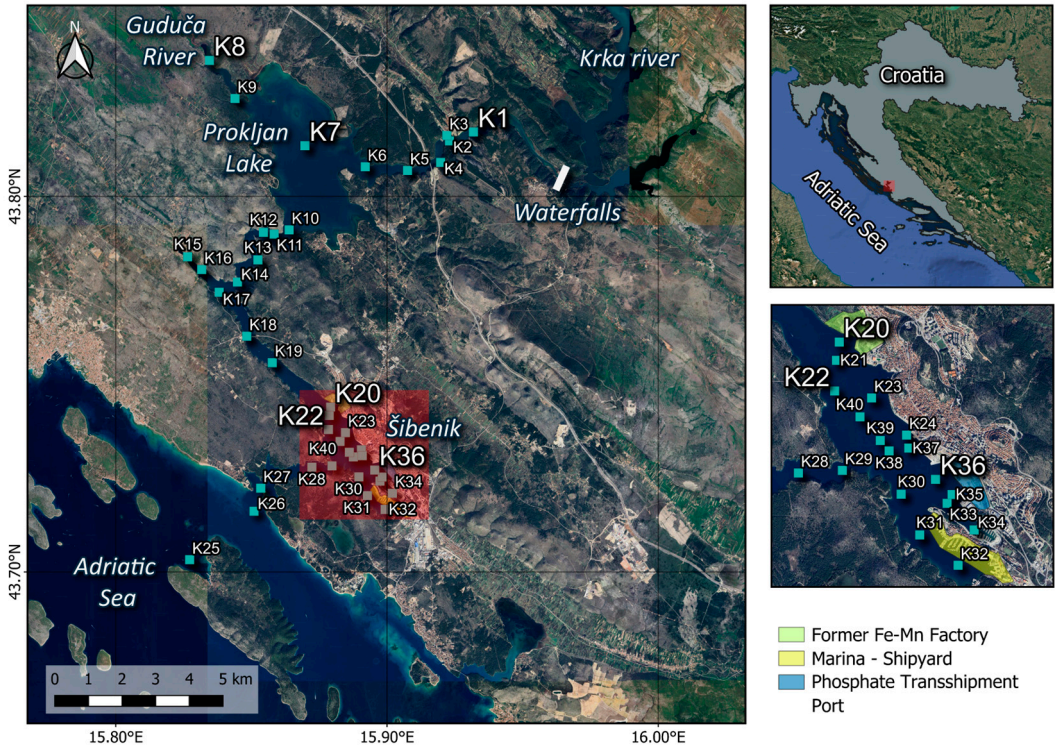

Figure 1. Map of the Krka River Estuary showing sediment sampling locations. Surface sediment sites are marked by turquoise squares with corresponding IDs. Sampling sites where sediment cores were also collected are indicated by enlarged site ID font sizes. The inset on the right, representing the area within the red rectangle, provides a magnified view of the city of Šibenik and Šibenik Bay for improved spatial resolution.

2.2. Sampling and Sediment Pretreatment

Surface sediment sampling was carried out in August and September 2016 throughout the Krka River Estuary, with higher sampling density in the lower part (Šibenik Bay) due to the history of anthropogenic pressures in that area, particularly near known sources of pollution such as port and industrial facilities. In the upper part of the estuary, which is rather pristine, sampling locations were selected to represent different sedimentation areas identified in previous research. Samples were collected at 36 locations (average sampling density of ~2 samples km^{-2}) using a gravity corer (Uwitec, Mondsee, Austria) equipped with PVC tubes (9 cm diameter, 50 cm length). The uppermost 5 cm of sediment was retrieved immediately on board. In the following year, six sediment cores were collected from selected sites (K1, K7, K8, K20, K22 and K36) to investigate historical contamination trends. The sampling depth of the sediment cores was determined by the specifications of the sampling equipment and the ability of the corer to penetrate the sediment of the karst Krka River estuary. Despite variations in the length of individual cores (11 to 36 cm), the cores obtained cover a significant chronological range due to the characteristically low sedimentation rates in the lower part of the Krka River estuary. As this study focuses on assessing the suitability of the MS method for rapid assessment of sediment metal contamination, rather than establishing a detailed geochronological record, the sampled depths were considered sufficient to validate the correlation between magnetic signals and metal concentrations. The sampling locations of sediment cores represent different estuarine sedimentation areas, ranging from carbonate-rich sedimentation influenced by the Krka River (K1) to mixed terrigenous–carbonate areas (K7, K8) and marine carbonate zones (K22) affected by industrial (K20) and port activities (K36). Cores were retrieved by a scuba diver using hand-driven Plexiglas corers, except at location K8,

where a gravity corer was used. Immediately after sampling, cores were transported to the laboratory and sliced at intervals of 1 or 2 cm. All samples were processed in the same manner. They were stored in high-density polyethylene (HDPE) containers and kept at −20 °C until further treatment. Initial laboratory treatment of samples included freeze-drying, sieving to <2 mm and grinding using a Planetary Ball Mill PM 100 (Retsch, Haan, Germany).

2.3. Sediment Analysis

2.3.1. Magnetic Susceptibility Measurements

The magnetic susceptibility of sediment samples was measured using an MS meter SM30 (ZH Instruments, Brno, Czech Republic). This highly sensitive device features an 8 kHz LC oscillator, a sensor with a large pick-up coil, and a sensitivity of 1×10^{-7} SI units. Owing to its sensor design, the instrument can obtain 90% of the magnetic signal from the upper 20 mm of the sample, providing reliable readings even on uneven surfaces. The instrument can measure various materials, including diamagnetic substances such as limestone and quartz [47]. In this study, each sediment sample was measured in triplicate, and the final MS value was recorded as the arithmetic mean of these three readings. Results are shown in 1×10^{-3} SI units.

2.3.2. Multielemental Analysis

The elemental concentrations of the sediment samples used in this study were previously analysed and described by Cukrov et al. [52,53]. The datasets from those papers were used here for comparison with magnetic susceptibility measurements. Briefly, semi-total concentrations of the sediment samples were determined using high-resolution inductively coupled plasma mass spectrometry (HR ICP-MS, Element 2, Thermo, Bremen, Germany). For analysis, 100 mg of sediment was digested with 10 mL of aqua regia (2.5 mL HNO_3 and 7.5 mL HCl, Trace Analysis grade, Fisher Scientific, Waltham, MA, USA) as described in detail in Cukrov et al. [53] for sediment cores and in Cukrov et al. [52] for surface sediment. For validation of the digestion method, in both cases, a PACS-2 (National Research Council of Canada, Ottawa, ON, Canada) certified reference material was used.

2.3.3. X-Ray Powder Diffraction (XRD) Analysis

To provide a representative insight into the qualitative mineralogical composition of the sediments from the six sampled cores and to optimise analytical resources, 19 of the 80 subsamples were selected for X-ray powder diffraction (XRD) analysis. The selection was based on visual lithological inspection and the results of geochemical and granulometric (not presented here) analyses. The mineralogical composition of sediment was determined in the following sediment core subsamples (K1 (0–2 cm, 12–14 cm, 22–24 cm, 34–36 cm), K7 (0–2 cm, 34–36 cm), K8 (0–2 cm, 12–14 cm, 18–20 cm, 24–26 cm), K20 (0–2 cm, 8–10 cm, 14–16 cm, 20–22 cm), K22 (0–1 cm) and K36 (0–2 cm, 4–6 cm, 10–12 cm, 16–18 cm)) on a Philips X'Pert Pro instrument (Philips Analytical, Almelo, The Netherlands) using CuKα radiation. The experimental conditions were as follows: 40 kV, 40 mA, step size 0.02° 2θ, step time 1 s, and scanned range 4–63° 2θ. Mineral phases were identified using X'Pert HighScore software (version 2.1, PANalytical, Almelo, Netherlands) by comparing the obtained experimental data with standard reference patterns.

2.4. Statistical Analysis

Statistica 6.0 software (StatSoft, Tulsa, OK, USA) was used to perform all statistical analyses in this research. The following statistical methods were selected to best describe the behaviour of the studied parameters in the Krka River Estuary.

Basic statistical parameters (N (number of cases), mean, median, minimum, maximum, range, standard deviation) were determined to provide a brief overview of the measured values, without presenting the entire, very large dataset, which is available in the supplement.

Statistical anomalies were determined using the boxplot method, based on normal or lognormal boxplots, which were constructed based on empirical cumulative distribution plots. Anomaly detection is one of the most important statistical tools in pollution studies, as large anomalies usually indicate anthropogenic influence. The box length represented the interquartile range. Outlier values (which present statistical anomalies of a lower degree) are defined as those between 1.5 and 3 box lengths from the upper or lower edge of the box. Extreme values (anomalies of a higher degree) are defined as those more than 3 box lengths from the edge of the box [54,55].

Correlation statistical analysis was performed using calculation of Pearson's correlation coefficient and it is presented as a correlation matrix to enable determination of the strength of linear correlation of mass fractions between the studied elements. A total of 28 measured elements were included in the correlation matrix to provide insight into all potential relationships between magnetic susceptibility and sediment elemental composition. The calculated values were statistically significant at $p < 0.05$. The reasons for using Pearson's correlation coefficient are described in detail later in Section 3.2.

Cluster analysis is a multivariate statistical method that represents a hierarchical approach [56]. Q-mode cluster analysis seeks clusters of similar samples. It was performed to get groups of similar samples. In interpreting our results, it is important to determine whether samples from a specific cluster are linked to a particular part of the estuary and whether a sample belonging to a particular cluster may indicate potential anthropogenic influence.

Factor analysis was applied to reduce variable complexity (number of variables) and to identify key natural or anthropogenic influences, assuming that correlations between multiple elements are driven by a smaller set of main factors [57,58]. It was performed with Varimax rotation, and the dataset comprised the analytical results of 14 selected parameters: MS and 13 chemical elements (Li, Cd, Pb, Al, Cr, Mn, Fe, Co, Ni, Cu, Zn, Ba, and Hg). Factor analysis can also indicate which possible elemental associations are present in the studied samples and if they have anthropogenic or natural origins.

The study area map was created using QGIS version 3.44.8, while the other two maps in the manuscript were produced with Surfer 15 (Golden Software LLC, Golden, CO, USA). For the MS spatial distribution map, data from the surface sediment were used, and interpolation was performed using the inverse distance to a power algorithm (IDW). This interpolation method was selected to preserve spatial anomalies, rather than smoothing them as occurs with some other interpolation methods, such as Kriging. By using this approach, we ensured that the interpolation respected the measured values at the sample locations and maintained the sharp local variations that are crucial for identifying significant geochemical and environmental anomalies in the MS data.

3. Results and Discussion

3.1. Spatial Distribution and Statistical Characterisation of MS in the Surface Sediments of the Krka River Estuary

Magnetic susceptibility (MS) was measured in two datasets: (i) surface sediments from the Krka River Estuary and (ii) six sediment cores, which were collected to observe the behaviour of MS and element distribution at different depths. The results of MS measurements for surface sediments from the Krka River Estuary are presented in Figure 2 and Table S1. The MS measured in sediment cores is not presented here to avoid duplication, as it will be shown later as charts and discussed in detail.

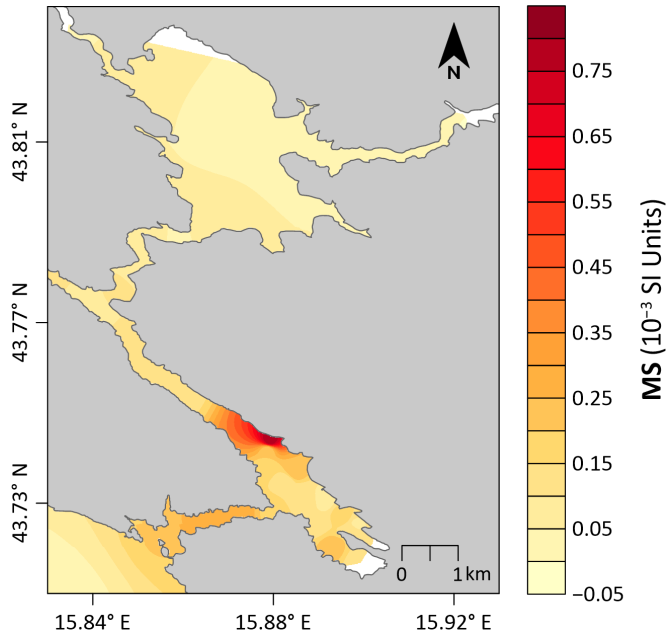

Figure 2. Contour map showing the spatial distribution of magnetic susceptibility (MS) in the surface sediments of the Krka River Estuary.

Figure 2 presents a contour map, showing the spatial distribution of MS in the surface sediments of the Krka River Estuary. As can be seen from this map, lowest values of MS (<0.05 × 10^{-3} SI units) prevail in the most upstream part of the estuary. Values are slightly higher (0.05–0.15 × 10^{-3} SI units) in the part of canyon between southern part of Prokljan Lake and Šibenik town, while around Šibenik town and its port and industry, values are very much elevated, with the highest measured value of 0.799 × 10^{-3} SI units. In the St. Ante Channel, most downstream part of the Krka River Estuary, linking Šibenik with open sea, MS values are approximately 0.25–0.35 × 10^{-3} SI units, while going towards the open sea they are gradually decreasing. The spatial distribution of MS values in surface sediments is highly important, as the spatial distribution of several metals, especially Mn, Pb, Ba, and Sb, closely resembles the MS distribution. Therefore, a spatial map of MS distribution can be very useful for identifying potentially toxic metal hotspots in the studied region, as elevated heavy metal values usually correspond with the highest MS values.

To get a better insight into results, basic statistical parameters (N-number of cases, Mean, Median, Minimum, Maximum, Range and Standard Deviation) were calculated for surface sediments of the Krka River Estuary and are presented in Table 1.

Table 1. Basic statistical parameters of magnetic susceptibility (MS) measured in surface sediments of the Krka River Estuary.

	Valid N	Mean	Median	Min	Max	Range	Std. Dev.
MS	36	0.123	0.106	−0.001	0.799	0.800	0.136

The mean MS value in the Krka River Estuary is quite low compared to some other sites in Croatia; for example, in Zagreb city soils the mean value is 0.374 [47], whereas in Sisak city soils the mean value is much higher at 18.6 [59]. Study of Frančišković-Bilinski et al. [60] reported values for karstic and flysch rivers of Slovenia and part of Croatia. Mean value of rivers from old Celje industrial region in Slovenia is 1.30×10^{-3} SI units, for Slovenian clean karstic rivers 0.479×10^{-3} SI units and for Croatian and Slovenian flysch and alogene rivers 0.340×10^{-3} SI units. So, median values of all three groups of rivers from that study are much higher than median from the Krka River Estuary. Also, it is interesting to compare that maximal value measured in the Krka River Estuary is significantly lower than median value from the Celje industrial region, which indicates that Krka River Estuary is much less polluted than compared region.

We can further note that the difference between the median and the mean value exists, but it is not that large, which means that the distribution is not too irregular, and this small irregularity is a consequence of that one rather large anomaly in the K20 sample. If we exclude this large anomaly from dataset, rest of the samples have a very regular distribution. The minimum value is extremely low, even slightly negative. Negative magnetic susceptibility in sediments is usually caused by the presence of diamagnetic minerals (such as carbonates and opal) and the absence of strong magnetically minerals (such as magnetite), which repel, rather than attract, magnetic fields. The XRD analysis (Figure S1) confirmed the predominance of calcite in the uppermost part of the estuary (K1), providing a mineralogical explanation for the very low MS values, as carbonate minerals are diamagnetic and therefore contribute to negative MS. The prevalence of carbonate minerals in this part of the estuary is not surprising, given that the Krka River brings very little terrigenous material, which could otherwise supply a higher amount of magnetic minerals. At this site, pyrite was detected in the sediment. However, pyrite is only weakly paramagnetic, and its formation (pyritisation) typically occurs under anoxic conditions where sulphate-reducing bacteria consume ferromagnetic minerals such as magnetite. Therefore, in the uppermost part of the estuary, even if minor amounts of iron oxides were originally present, their transformation into weakly magnetic pyrite, combined with the prevalence of diamagnetic carbonates, effectively erases the magnetic signature.

Statistical anomalies of MS values of surface sediments from Krka River Estuary were determined using boxplot method, which is presented in Figure 3. As we can see from the boxplot, statistically speaking, there is only one anomaly present, a rather pronounced extreme with an MS value of 0.799×10^{-3} SI units in sample K20. Therefore, it can be assumed that this sample contains elevated values of some of the heavy metals. All other samples have a very regular distribution and therefore it is to be expected that there is no (at least not significant) anthropogenic influence in them, especially because MS values are not high.

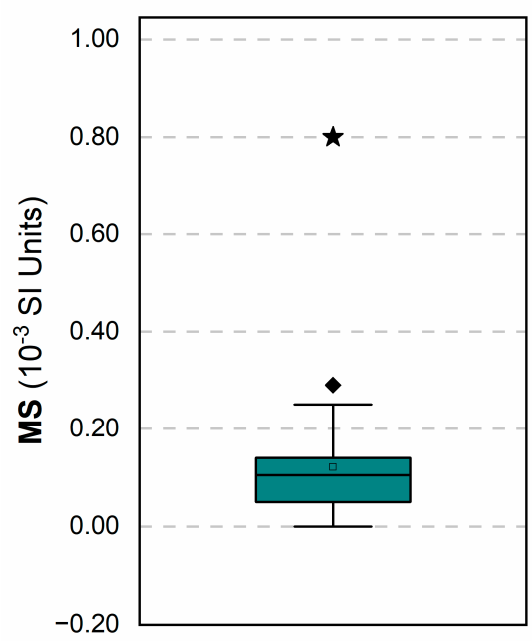

Figure 3. Statistical anomalies in MS values of surface sediments from the Krka River Estuary, determined using the boxplot method. The mean value is marked with an empty square symbol, the extreme value with a black star symbol, while the outlier is indicated by a black diamond symbol.

Sample K20, which statistically presents a very large anomaly, does not actually have an absolutely very high MS value: for example, in the Zagreb city area the values range up to 3×10^{-3} SI units [47], and in Sisak area, which is strongly polluted with Fe particles from metallurgic industry, they go up to 100×10^{-3} SI units [59]. Therefore, anomaly K20 was not excluded from all analyses performed within statistical evaluation, as its influence on elevation of some parameters, e.g., Mean or Median, was not significant. However, given its anomaly compared to other samples, it is to be expected that sample K20 is very likely under anthropogenic influence and that certain heavy metals are significantly elevated there. Therefore, when using magnetic susceptibility to assess sediment metal contamination, it is crucial to consider the natural MS values in the study area and to examine in detail the spatial zones where they are elevated.

3.2. Determining Correlations Between MS and Studied Elements in Surface Sediments of the Krka River Estuary

A correlation analysis was conducted to determine the relationships between measured MS values and 28 chemical elements studied in the Krka River Estuary. The complete correlation matrix is presented in Table S2, while significant correlations between MS and the elements are shown in Table 2. The Pearson correlation coefficient was used because the vast majority of our data are normally distributed. The Pearson correlation coefficient is superior to Spearman's in the case of continuous, normally distributed data. Its linear relationship provides greater precision, sensitivity to exact values, and better suitability for predictive modelling. The main difference from the Spearman coefficient is that Pearson measures the strength of raw values, whereas Spearman only analyses rankings [61]; therefore, Pearson is much more precise in cases similar to ours.

Table 2. Significant correlations ($p < 0.05$) between magnetic susceptibility measurements (MS) and studied elements in surface sediments of the Krka River Estuary.

	Sn	Sb	Pb	Bi	Mn	Fe	Co	Ni	Cu	Zn	Ba
MS	0.39	0.71	0.87	0.43	0.88	0.38	0.73	0.40	0.44	0.38	0.76

The results of the correlation analysis indicate that MS is an effective proxy for identifying spatial variability and metal enrichment in sediments of the Krka River Estuary. Statistically significant correlations were found for several elements, with the strongest relationships observed for Mn (r = 0.88) and Pb (r = 0.87), followed by Ba (0.76), Co (0.73), and Sb (0.71). These high correlation coefficients are at the upper end of values recorded in similar studies worldwide (Table 3), suggesting a specific mechanism of metal input into this system.

Table 3. Examples of MS–metal correlation patterns in sediments and soils.

Study/Site	Main MS–Metal Pattern	Interpretation	Citations
Vistula estuary (Baltic)	Moderate MS correlations with Cd, Cu, Pb, Zn (rs ≈ 0.4–0.6); weak/insignificant with Cr, Fe	MS reflects technogenic enrichment, mediated by grain size and organic matter	[11]
Inner Ambon Bay	Strong positive MS–Cr/Co/Ni/Mn correlations (R ≈ 0.64–0.90)	MS reliable proxy for Cr, Co, Ni, Mn contamination in many sites	[16]
Kerala coast	Significant MS correlations with V, Zn, Mn, Ba, As, Pb	Indicates impact of anthropogenic magnetic particulates on these elements	[14]
Iran soils	Strong MS–Fe, Mn, Zn, Ni, Co, Cr correlations (r up to 0.9)	MS useful for semi-quantitative metal estimation in natural systems	[62]

The strong association of MS with Mn and Pb directly reflects the ecological history of the lower part of the estuary. Previous research indicates that elevated concentrations of these elements are primarily related to the historical activity of the former TEF factory in Šibenik [53]. The production of ferromanganese and silicomanganese generated significant amounts of slag and particles from electrofilters (so-called fly ash). Multielement analysis of slag collected from the former factory site confirmed a marked enrichment in numerous elements, especially manganese (Mn) [52,63]. These findings support the thesis that slag particles, transported by aeolian or hydrodynamic processes, were deposited in the surrounding estuarine sediments, thus directly influencing their geochemical composition. Interestingly, the correlation between MS and total iron (Fe) is relatively weak (r = 0.38), although statistically significant. The weak MS–Fe correlation, despite Fe's magnetic role, is consistent with other systems where Fe occurs mainly in non-magnetic or weakly magnetic phases and the "magnetic" fraction is carried by specific Fe-bearing minerals or technogenic particles rather than bulk Fe content [11,22,23,64]. Although iron is the most common ferromagnetic element, MS often shows much stronger correlations with other elements, such as Zn, Cu, or Ni, in various types of samples [11,62,65,66]. This is especially true where Fe is present in non-magnetic forms, such as silicate lattices, rather than as free oxides (like magnetite). Therefore, MS can also be used as a proxy for other heavy metal pollution (Zn, Cu, Cr, Pb) besides iron. MS can have the strongest correlations with these elements because they are deposited alongside the magnetic particles that provide the magnetic response. Thus, it can be assumed that MS often traces pollution more directly than total iron content. MS is primarily affected by the amount of ferrimagnetic minerals

(such as magnetite) rather than total iron, which is usually found in the form of paramagnetic minerals like hematite or pyroxenes [67,68]. Additionally, some elements like Zn and Cr can be incorporated into the lattice of other magnetic minerals, such as sphalerite, contributing to magnetic variability. Therefore, our finding that MS correlations in the Krka River estuary are significantly higher with other potentially toxic metals than with Fe is not unusual and is fully consistent with the literature.

The fact that correlations with Mn and Pb are twice as strong as those with Fe confirms that MS in Krka is a "selective indicator" of TEF industrial waste. Comparison with other systems (e.g., Vistula estuary or Kerala coast) shows that correlations in Krka (especially for Mn and Pb) are among the highest recorded. While in other systems MS often reflects mixed signals (grain size, organic matter), here the correlation is clear and direct. The presence of non-negligible but sub-significant correlations with Cr and As (>0.30) reflects findings that metals with mixed lithogenic and anthropogenic origins often show moderate MS relationships [12,16,69]. A recent paper on the Krka River Estuary highlighted that Cr and As in the estuary are predominantly of natural, terrigenous origin, but with a possible additional anthropogenic contribution in the Šibenik Bay area [52]. Therefore, the moderate associations of Cr and As with MS may reflect the mixing of a natural detrital signal with local anthropogenic influences. This confirms that metals of mixed (lithogenic and anthropogenic) origin are also partially associated with the magnetic fraction. The results confirm that the MS measurement method in the Krka River Estuary is an extremely reliable tool for the rapid and economical detection of pollution hotspots. As MS measurements do not require expensive or time-consuming chemical sample preparation, they can serve as a primary tool for monitoring and spatial mapping of industrial waste distribution in the sediments of this protected area.

3.3. Source Identification of Metals in Krka River Estuary Sediments Using Multivariate Statistical Approaches

A Q-mode cluster analysis was performed, which included all parameters (MS and all studied elements). The cluster analysis in this work is based on Euclidean distance. This method groups data points by calculating the straight-line distance between them, defined as the square root of the sum of squared differences between their coordinates. It is important because it identifies clusters of high similarity, although it is sensitive to outliers [70]. As our dataset contains few statistical anomalies, it is well suited to this type of statistical analysis. Euclidean distance is used when cluster compactness is a priority and is a powerful, standard, and highly intuitive distance metric.

The results are presented in Tables 4–7 and Figure 4. Table 4 shows the Euclidean distances between clusters, Table 5 shows the cluster means, Table 6 lists the members of Cluster 1 with their distances from the corresponding cluster center, and Table 7 lists the members of Cluster 2 with their distances from the corresponding cluster center. In Figure 4 is presented spatial distribution of those two clusters. Based on their similarity, cluster analysis classified each sample into one of these two clusters, which clearly reflect the two basic sedimentological/geochemical areas of the estuary. Cluster 1 is characterized by very low MS values and lower concentrations of almost all elements, while Sr is higher in this group. In contrast, Cluster 2 shows higher MS values and significantly higher concentrations of most elements. This differentiation is robust and can be interpreted as a clear distinction between sediment with dominant biogeocarbonate sedimentation and sediment enriched with terrigenous and anthropogenically derived particles. The elevated Sr in Cluster 1 is consistent with predominant marine sedimentation, as it is well established in the geochemical literature that Sr is incorporated into marine carbonates and that its content in carbonate sediments can increase with the proportion of certain marine carbonate phases. Such an interpretation aligns with current knowledge about sedimentation in the

Krka River Estuary, with different areas of sedimentation, predominantly biogeocarbonate sedimentation in the lower estuary and the uppermost estuary and mixed sedimentation in the upper-middle area, where there is a greater influence of terrigenous material. Also, the map from Figure 4 visually confirms our interpretation that Cluster 1 is linked to dominant biogeocarbonate sedimentation, while Cluster 2 is linked to terrigenous and anthropogenically derived particles. In karst estuaries, the sediment is dominated by diamagnetic or weakly magnetic carbonate material, and even relatively small contributions of ferrimagnetic and industrial particles can produce a clearly measurable increase in MS, which enables the application of MS method as a rapid screening tool for metal enrichment in sediment, provided local geochemical conditions and site-specific MS values are established.

Table 4. Euclidean distances between clusters.

	Cluster 1	**Cluster 2**
Cluster 1	0.000	13,314,850
Cluster 2	3648.952	0

Table 5. Cluster means (for MS in 10^{-3} SI units, for elements in mg kg^{-1}).

	Cluster 1	**Cluster 2**
MS	0.08	0.14
Li	30.50	51.66
Be	1.03	1.79
Rb	35.63	64.07
Mo	1.55	1.85
Ag	0.29	0.58
Cd	0.67	1.13
Sn	4.77	7.88
Sb	0.53	0.73
Cs	3.10	5.37
Tl	0.40	0.64
Pb	47.78	126.36
Bi	0.74	1.89
U	2.94	3.88
Al	22,902.35	39,897.89
Ti	779.26	1363.11
V	50.19	81.82
Cr	48.75	81.42
Mn	531.63	2277.61
Fe	14,057.99	23,736.34
Co	5.22	8.66
Ni	30.09	50.21
Cu	23.62	54.67
Zn	114.64	254.53
Sr	1255.78	826.98
Ba	92.33	183.20
As	10.08	15.44
Pt	0.02	0.03
Hg	0.51	1.61

Table 6. Samples assigned to Cluster 1 with their distances from respective cluster center.

	Distance
K02	653.794
K03	823.982
K04	1066.568
K05	969.291
K11	1336.126
K13	535.862
K25	1028.556
K28	1063.829
K29	672.731
K30	1348.526
K35	635.450
K40	1602.134

Table 7. Samples assigned to Cluster 2 with their distances from respective cluster center.

	Distance
K06	1805.288
K07	619.853
K08	933.193
K09	1895.161
K10	696.893
K12	569.635
K14	1820.565
K15	2399.776
K16	1506.551
K17	486.411
K18	891.493
K19	2561.997
K20	5579.231
K21	281.511
K22	143.491
K23	206.603
K31	1316.874
K32	962.485
K33	411.562
K34	664.538
K36	1670.390
K37	1130.563
K38	864.647
K39	548.979

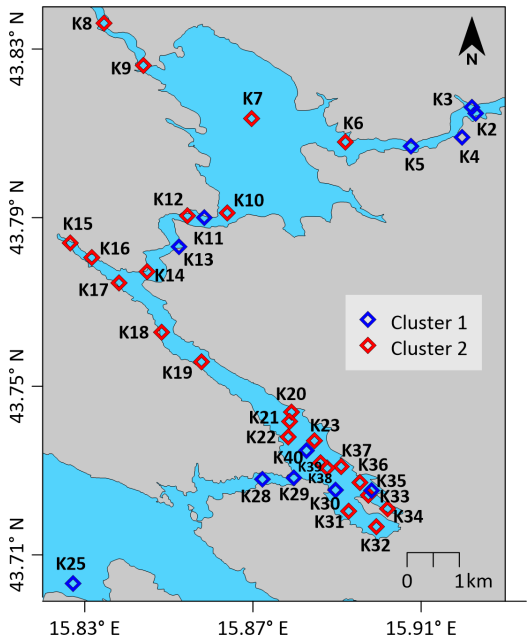

Figure 4. Spatial distribution of the two primary groups identified by performing Q-mode cluster analysis on the magnetic susceptibility (MS) dataset from Krka River Estuary surface sediments.

Furthermore, Factor analysis was performed on 14 parameters (MS, Li, Cd, Pb, Al, Cr, Mn, Fe, Co, Ni, Cu, Zn, Ba, and Hg) to provide better insight into possible elemental and mineral associations, the origin of elements, and the relationships between them. The results are presented in Figure 5, which shows the factor loadings, and in Table 8, which presents the factor scores for each sample. The factor analysis revealed that 87.91% of the total variability can be explained by the first three factors, which is a very good result. Generally, the higher the factor scores of a factor in a given sample, the more dominant that factor is in that sample. This high variance extraction indicates a strong and significant differentiation of geochemical processes within the Krka River Estuary.

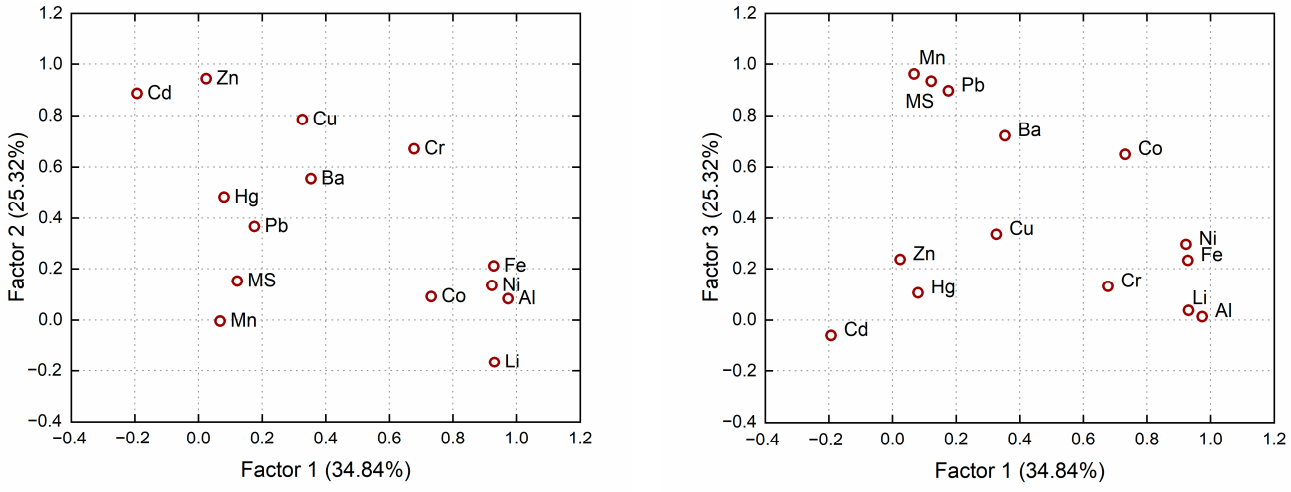

(**a**) (**b**)

Figure 5. Factor loading plots for the magnetic susceptibility (MS) and 13 elements analyzed in the surface sediment samples of the Krka River Estuary. The plots represent: (**a**) Factor 1 versus Factor 2; (**b**) Factor 1 versus Factor 3.

Table 8. Computed factor scores based on Factor analysis with Varimax normalized rotation.

	Factor—1	Factor—2	Factor—3
K02	−1.43202	−0.511458	−0.430989
K03	−0.74233	−0.352740	−0.500716
K04	−1.61448	−0.643527	−0.346960
K05	−0.73301	−0.639139	−0.400579
K06	−0.22616	−0.655310	−0.502306
K07	0.62162	−0.664367	−0.567896
K08	0.10121	−0.352488	−0.678330
K09	1.41087	−0.440513	−0.647518
K10	0.83565	−0.639147	−0.536149
K11	−1.79931	−0.804547	−0.173973
K12	0.68181	−0.671038	−0.439683
K13	−0.90869	−0.734280	−0.211154
K14	1.48331	−0.493228	−0.362374
K15	1.52149	0.141073	−0.318623
K16	−0.19305	−0.603315	−0.229250
K17	0.50059	−0.073169	−0.313946
K18	0.96346	−0.477680	−0.223900
K19	1.85033	−0.328211	−0.203550
K20	0.07754	−0.085641	5.503177
K21	0.75203	−0.212625	0.442555
K22	0.65829	−0.178986	0.183156
K23	0.65557	0.099730	0.472313
K25	−1.48376	−0.654558	−0.270219
K28	−1.42755	−0.650259	0.517350
K29	−0.79018	−0.564371	0.268957
K30	−0.48097	0.250132	0.235693
K31	−0.07923	0.710719	0.308931
K32	0.25623	1.461062	0.025969
K33	0.46573	1.289889	−0.240629
K34	0.61225	1.001129	−0.052748
K35	−1.93245	0.673888	−0.184467
K36	−0.86757	4.605266	−0.569120
K37	0.27897	0.994124	0.064399
K38	0.40332	0.434335	0.249304
K39	0.70569	0.096313	0.040058
K40	−0.12519	−0.327064	0.093218

Factor 1 showed very strong correlations with Li, Al, Fe, Co, and Ni, and can be attributed to the natural geological background. A strong loading of typical terrigenous elements coincides with the input of detrital material into the estuary. This agrees with previous findings that link the lithogenic elements in the sediments of the Krka River Estuary to the Guduča River and the Litno spring, which carry flysch and flysch-like deposits into the estuary. Factor 2 is related to Cd, Cu, and Zn, and can be interpreted as an anthropogenic factor associated with activities within Šibenik Bay, including wastewater, port, and shipyard operations. Factor 3 is associated with MS, Pb, Mn, and Ba. The grouping of MS with Pb, Mn, and Ba provides statistical confirmation that MS in this area is a reliable indicator of sediment enrichment with metals resulting from industrial activities. The exceptionally high factor values at the sampling sites near the abandoned TEF factory confirm the existence of local pollution hotspots caused by the factory's many years of operation.

The strong loading of MS on Factor 3 (0.93) indicates that in the Krka River Estuary, MS is not only an indicator of sediments with a higher detrital component, but also an effective proxy for anthropogenically induced particles. This is consistent with other case studies where magnetic parameters are used to identify hotspots of industrial sediment contamination. As observed in other systems (e.g., Vistula Estuary or Ambon Bay), MS is a strong indicator for specific metals (Mn, Pb, Ba, Co), while it remains a weaker indicator for others (Fe, Cr, As) [11,16]. Therefore, when conducting environmental magnetism studies, it should always be considered that MS reflects specific mineral phases rather than overall sediment chemistry. The clear distinction between the terrigenous factor (Factor 1) and the industrial factor (Factor 3) demonstrates that MS integrates both lithogenic inputs and technogenic particles. In the Krka estuary, the low natural magnetic background makes the anthropogenic signal from the TEF slag, which is rich in Mg and Pb, stand out with high contrast.

Although MS is very effective, it is not a universal replacement. The weak correlation between MS and total Fe, in combination with the lack of a stronger link between elements such as Cd, Cu and Zn, highlights the need of considering local mineralogical and geochemical contexts when interpreting MS results. However, as a targeted tool for the identification of Mn and Pb enrichment associated with the ferroalloy industry, MS proves to be an extremely sensitive and operationally valuable method. This integrated approach—combining MS with multivariate statistics—places the Krka River Estuary as a well-characterized case study within the global research on environmental magnetism.

3.4. Vertical Distribution of MS Within Layers in Sediment Cores from the Krka River Estuary

To gain better insight into the behaviour of MS with increasing sediment depth, six sediment cores from the Krka River Estuary were analysed. All layers from each core were statistically evaluated separately. The boxplot method was used to identify any anomalies within each core. Only core K1 was found to contain anomalies; all other cores showed no statistical MS anomalies and exhibited a regular natural distribution. Therefore, their boxplots are not presented here. In core K1, two pronounced extremes were observed in the 12–14 cm and 20–22 cm layers, and one outlier was found in the 22–24 cm layer. The results of the boxplot analysis for core K1 are shown in Figure 6.

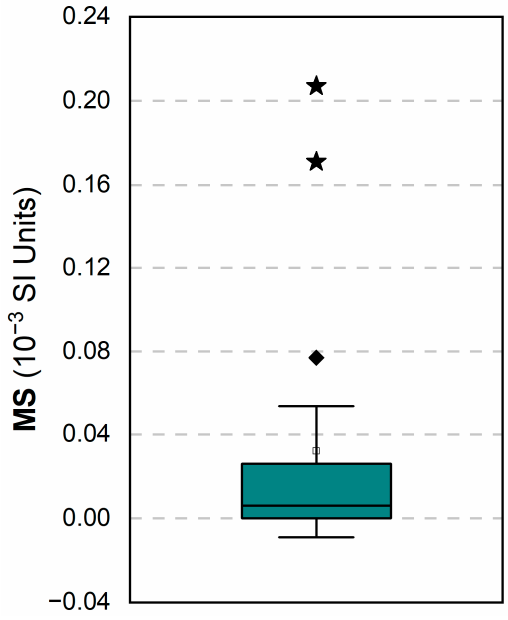

Figure 6. Statistical anomalies in MS values of the sediment core K1 from the Krka River Estuary, determined using the boxplot method. The mean value is marked with an empty square symbol,

the extreme values with a black star symbol, while the outlier is indicated by a black diamond symbol.

In core K1, the most upstream studied location in the estuary, all MS anomalies, as well as other highest values, are present approximately in the middle of the core, at depths from about 12 to 24 cm (Figure 7). In most of the shallower layers, MS values are very low, indicating a decrease in contamination in more recent years. According to Cukrov et al. [50], the sedimentation rate upstream of Prokljan Lake is 2 mm year^{-1}, so it can be assumed that these elevated MS values originate from layers that are 60–120 years old. However, differences in MS values between these layers are very high. Therefore, it seems there was no continuous input of heavy metal contamination, but rather some sporadic events during that period brought contamination.

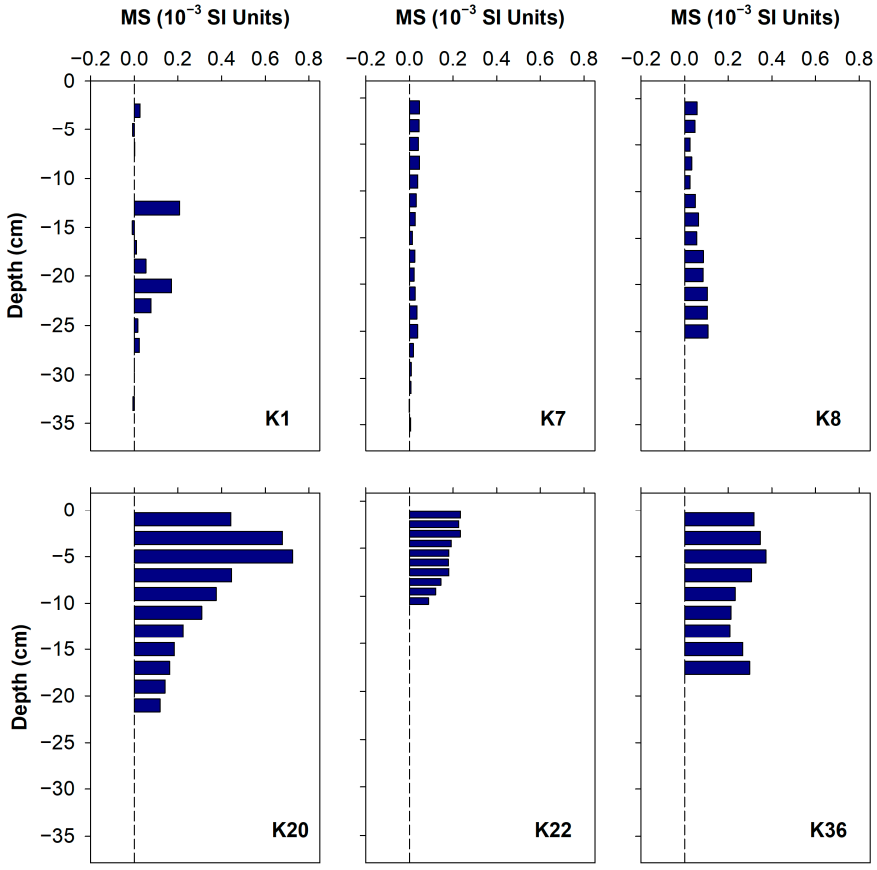

Figure 7. Distribution of magnetic susceptibility (MS) values within each of 6 studied sediment cores from the Krka River Estuary.

In core K7, located in the middle of Prokljan Lake, a trend of decreasing MS values is observed from the surface to 16 cm depth, after which an increase is visible up to 26 cm, followed by another decline (Figure 7). However, these changes in MS values are not large. In layers deeper than 26 cm, values are very low. According to Cukrov et al. [50], the average sedimentation rate in Prokljan Lake is 4 mm year^{-1}, so these very low values start in layers older than approximately 65 years.

In core K8, located in Prokljan Lake at the Guduča River inflow, a significant decrease in MS values is observed from the deepest layers to about 4–6 cm, and from there to the surface, MS increases slightly again, but remains significantly lower than in the deeper layers (Figure 7). At this location, according to Cukrov et al. [50], annual sedimentation is about 5 mm, so this slight increase in MS values occurs in layers 8–12 years old.

Anthropogenic influence at this location is unlikely, so the increased MS values most probably originate from terrigenous particles brought by the Guduča River. The rather small differences between layers (years) are most likely the result of changes in the quantity of material brought by the Guduča River, which mostly depends on the precipitation rate.

In core K20, located just in front of the closed ferroalloys factory, the highest MS values are found in the 4–6 cm layer; from there, they decrease towards the surface and with depth (Figure 7). The sedimentation rate in Šibenik Bay is estimated to be less than 1 mm per year [50]; however, sediment near the former TEF factory is enriched with slag material. Therefore, it is not possible to assume continuous sedimentation in that area or to discuss the dynamics of contamination over the years. Nevertheless, the clear decreasing trend in the uppermost sediment possibly reflects the closure of the TLM factory and the remediation of the surrounding area.

In core K22, located near the Martinska marine station, just opposite K20, there is a noticeable trend of decreasing values towards deeper layers, indicating that anthropogenic influence at this location was gradually increasing over time (Figure 7). In the three shallowest layers, that increase has stopped and MS values are no longer rising; it is expected that they will start to decrease in the future, similar to core K20, but with some delay.

In core K36, located just in front of Šibenik harbour, the highest values are present in the 4–6 cm layer (Figure 7). They decrease slightly towards the surface and with depth, but in the two deepest layers, they increase slightly again. However, there are no very large differences in MS values in any layer of this core, indicating that anthropogenic influence at this location has remained about the same throughout the time span covered by this core.

Although results from the current study confirm that MS is a reliable tool for assessing metal enrichment in surface sediment of the karstic estuary, its application to sediment cores requires significant caution. When dealing with depth profiles, MS has several important limitations that make it a potentially ambiguous indicator. Lithology, particle size distribution, and early diagenetic processes have a dominant influence on vertical MS variations; therefore, separation of the magnetic signal from the actual metal concentrations can occur. MS can be useful for screening cores to select depths for further chemical analysis and for distinguishing broadly impacted intervals, but it is not robust enough to be used as a stand-alone method to quantify vertical metal enrichment or to discuss historical contamination input in the environment.

4. Conclusions

The current study on the Krka River Estuary has demonstrated that MS serves as an effective metal enrichment proxy even within karstic estuarine sediments, consistent with its successful application in other types of environments worldwide. In predominantly carbonate settings, which typically have low background MS, various anomalies can be directly attributed to anthropogenic inputs and elevated concentrations of potentially toxic elements, confirming the suitability of MS as a reliable tool for preliminary environmental screening. However, comparison with published data from both pristine karst areas and heavily polluted environments clearly indicates that MS values are highly site-specific and strongly influenced by local lithology and sedimentary conditions. Therefore, local background MS levels must always be established and carefully considered when interpreting pollution signals. Specifically, within the Krka River Estuary, the correlation matrix revealed that the strongest correlation (up to 0.88) is with manganese, followed by lead (0.87), barium (0.76), cobalt (0.73), and antimony (0.71). Correlations with other elements, such as iron (0.38), are considerably weaker, though still statistically significant.

Owing to its low cost, simplicity, and speed, MS screening is particularly promising for use in low-income regions, where it can serve as an initial step in optimising monitoring strategies by identifying hotspots and prioritising sites for subsequent, more expensive and precise geochemical and speciation analyses. In this way, magnetic susceptibility can play a key role as a practical first-line tool in the integrated assessment of sediment quality and sustainable management of estuarine and coastal environments, including sensitive karst systems such as the Krka River Estuary.

Supplementary Materials: The following supporting information can be downloaded at: https://www.mdpi.com/article/10.3390/environments13050258/s1, Figure S1: X-ray diffraction (XRD) patterns of selected bulk sediment subsamples of sediment cores from the Krka River Estuary. Each panel represents a vertical profile of a single core, showing the mineralogical composition at different depth intervals. Mineral abbreviations: Ap-apatite, Arg-aragonite, Cal-calcite, Dol-dolomite, Fs-feldspar, Hl-halite, Ill/Ms-Illite/Muscovite, Mg-Cal-high-magnesian calcite, Py-pyrite, Qtz-quartz; Table S1: Results of MS measurements (10^{-3} SI units) in surface sediments of the Krka River Estuary; Table S2: Pearson correlation matrix for MS and elements measured in the surface sediment from the Krka River Estuary.

Author Contributions: Conceptualization, S.F.-B.; methodology, S.F.-B. and N.C. (Nuša Cukrov); validation, S.F.-B., N.C. (Neven Cukrov) and N.C. (Nuša Cukrov); formal analysis, S.F.-B.; investigation, S.F.-B., N.C. (Neven Cukrov) and N.C. (Nuša Cukrov); resources, S.F.-B. and N.C. (Neven Cukrov); data curation, S.F.-B. and N.C. (Nuša Cukrov); writing—original draft preparation, N.C. (Nuša Cukrov); writing—review and editing, S.F.-B. and N.C. (Neven Cukrov); visualization, N.C. (Nuša Cukrov). All authors have read and agreed to the published version of the manuscript.

Funding: This research received no external funding.

Data Availability Statement: The original contributions presented in this study are included in the article/Supplementary Materials. Further inquiries can be directed to the corresponding author(s).

Conflicts of Interest: The authors declare no conflicts of interest.

Abbreviations

The following abbreviations are used in this manuscript:

MS	Magnetic susceptibility
HDPE	High-density polyethylene
HR ICP-MS	High-resolution inductively coupled plasma mass spectrometry
XRD	X-ray powder diffraction
TEF	Electrode and Ferroalloy Factory

References

1. Thompson, R.; Oldfield, F. *Environmental Magnetism*; Springer: Dordrecht, The Netherlands, 1986.
2. Oldfield, F.; Hunt, A.; Jones, M.D.H.; Chester, R.; Dearing, J.A.; Olsson, L.; Prospero, J.M. Magnetic Differentiation of Atmospheric Dusts. *Nature* **1985**, *317*, 516–518. https://doi.org/10.1038/317516a0.
3. Hay, K.L.; Dearing, J.A.; Baban, S.M.J.; Loveland, P. A Preliminary Attempt to Identify Atmospherically-Derived Pollution Particles in English Topsoils from Magnetic Susceptibility Measurements. *Phys. Chem. Earth* **1997**, *22*, 207–210. https://doi.org/10.1016/S0079-1946(97)00104-3.
4. Strzyszcz, Z. Magnetic Susceptibility of Soils in the Areas Influenced by Industrial Emissions. In *Soil Monitoring*; Birkhäuser: Basel, Switzerland, 1993; pp. 255–269.
5. Strzyszcz, Z.; Magiera, T.; Heller, F. The Influence of Industrial Immissions on the Magnetic Susceptibility of Soils in Upper Silesia. *Stud. Geophys. Geod.* **1996**, *40*, 276–286. https://doi.org/10.1007/BF02300743.
6. Heller, F.; Strzyszcz, Z.; Magiera, T. Magnetic Record of Industrial Pollution in Forest Soils of Upper Silesia, Poland. *J. Geophys. Res. Solid Earth* **1998**, *103*, 17767–17774. https://doi.org/10.1029/98JB01667.

7. Plater, A.J.; Ridgway, J.; Appleby, P.G.; Berry, A.; Wright, M.R. Historical Contaminant Fluxes in the Tees Estuary, UK: Geochemical, Magnetic and Radionuclide Evidence. *Mar. Pollut. Bull.* **1999**, *37*, 343–360. https://doi.org/10.1016/S0025-326X(99)00052-1.
8. Kapička, A.; Petrovský, E.; Ustjak, S.; Macháčková, K. Proxy Mapping of Fly-Ash Pollution of Soils around a Coal-Burning Power Plant: A Case Study in the Czech Republic. *J. Geochem. Explor.* **1999**, *66*, 291–297. https://doi.org/10.1016/S0375-6742(99)00008-4.
9. Hanesch, M.; Scholger, R. Mapping of Heavy Metal Loadings in Soils by Means of Magnetic Susceptibility Measurements. *Environ. Geol.* **2002**, *42*, 857–870. https://doi.org/10.1007/s00254-002-0604-1.
10. Petrovský, E.; Ellwood, B.B. Magnetic Monitoring of Air- Land- and Water-Pollution. In *Quaternary Climates, Environments and Magnetism*; Cambridge University Press: Cambridge, UK, 1999; pp. 279–322.
11. Kusza, G.; Kubowicz, A.; Kłostowska, Ż.; Łuczak, K.; Łęczyński, L.; Hulisz, P. Environmental Effects of Potentially Toxic Elements and the Magnetic Susceptibility Distribution in the Surface Bottom Sediments in the Vistula Estuary (Gulf of Gdańsk, Poland). *J. Soils Sediments* **2023**, *23*, 3499–3512. https://doi.org/10.1007/s11368-023-03595-8.
12. Li, M.; Zhu, S.; Ouyang, T.; Tang, J.; Tang, Z. Magnetic Properties of the Surface Sediments in the Yellow River Estuary and Laizhou Bay, Bohai Sea, China: Implications for Monitoring Heavy Metals. *J. Hazard. Mater.* **2021**, *410*, 124579. https://doi.org/10.1016/j.jhazmat.2020.124579.
13. Hamdan, A.M.; Kirana, K.H.; Hakim, F.; Iksan, M.; Bijaksana, S.; Mariyanto, M.; Ashari, T.M.; Ngkoimani, L.O.; Kurniawan, H.; Pratama, A.; et al. Magnetic Susceptibilities of Surface Sediments from Estuary Rivers in Volcanic Regions. *Environ. Monit. Assess.* **2022**, *194*, 239. https://doi.org/10.1007/s10661-022-09891-z.
14. Kiruba, T.; Lakshmi Narasimhan, C.; Jayaprakash, P.; Juliet Josephine Joy, J.; Vidyasakar, A.; Ravisankar, R. Investigation of the Relation between Heavy Metal and Magnetic Susceptibility of Sediment from Kerala Coast for Contamination Study with Statistical Approach. *Int. J. Environ. Anal. Chem.* **2025**, *105*, 8056–8074. https://doi.org/10.1080/03067319.2025.2467171.
15. Devanesan, E.; Chandrasekaran, A.; Sivakumar, S.; Freny Joy, K.M.; Najam, L.A.; Ravisankar, R. Magnetic Susceptibility as Proxy for Heavy Metal Pollution Detection in Sediment. *Iran. J. Sci. Technol. Trans. A Sci.* **2020**, *44*, 875–888. https://doi.org/10.1007/s40995-020-00865-9.
16. Noya, Y.; Bijaksana, S.; Fajar, S.J.; Suryanata, P.B.; Harlianti, U.; Ibrahim, K.; Suandayani, N.K.T.; Multi, W.; Bahri, S. Magnetic Susceptibility in the Assessment of Toxic Heavy Metal Elements in the Surface Sediments of Inner Ambon Bay, Maluku Province, Indonesia. *Heliyon* **2024**, *10*, e27497. https://doi.org/10.1016/j.heliyon.2024.e27497.
17. Harikrishnan, N.; Chandrasekaran, A.; Ravisankar, R.; Alagarsamy, R. Statistical Assessment to Magnetic Susceptibility and Heavy Metal Data for Characterizing the Coastal Sediment of East Coast of Tamilnadu, India. *Appl. Radiat. Isot.* **2018**, *135*, 177–183. https://doi.org/10.1016/j.apradiso.2018.01.030.
18. Venkatachalapathy, R.; Veerasingam, S.; Basavaiah, N.; Ramkumar, T.; Deenadayalan, K. Environmental Magnetic and Geochemical Characteristics of Chennai Coastal Sediments, Bay of Bengal, India. *J. Earth Syst. Sci.* **2011**, *120*, 885–895. https://doi.org/10.1007/s12040-011-0108-z.
19. Li, X.; Yang, Y.; Yang, J.; Fan, Y.; Qian, X.; Li, H. Rapid Diagnosis of Heavy Metal Pollution in Lake Sediments Based on Environmental Magnetism and Machine Learning. *J. Hazard. Mater.* **2021**, *416*, 126163. https://doi.org/10.1016/j.jhazmat.2021.126163.
20. Pan, H.; Lu, X.; Lei, K.; Shi, D.; Ren, C.; Yang, L.; Wang, L. Using Magnetic Susceptibility to Evaluate Pollution Status of the Sediment for a Typical Reservoir in Northwestern China. *Environ. Sci. Pollut. Res.* **2019**, *26*, 3019–3032. https://doi.org/10.1007/s11356-018-3844-7.
21. Paramasivam, K.; Ramasamy, V.; Suresh, G.; Vimalathithan, R.M. Magnetic Susceptibility as Proxy for Metal Concentrations and Their Risk Levels in Vaigai River Sediment, Tamilnadu, India: Horizontal and Vertical Approach. *Soil Sediment Contam. Int. J.* **2024**, *33*, 594–611. https://doi.org/10.1080/15320383.2023.2226753.
22. Sudarningsih, S.; Pratama, A.; Bijaksana, S.; Fahruddin, F.; Zanuddin, A.; Salim, A.; Abdillah, H.; Rusnadi, M.; Mariyanto, M. Magnetic Susceptibility and Heavy Metal Contents in Sediments of Riam Kiwa, Riam Kanan and Martapura Rivers, Kalimantan Selatan Province, Indonesia. *Heliyon* **2023**, *9*, e16425. https://doi.org/10.1016/j.heliyon.2023.e16425.
23. Mariyanto, M.; Amir, M.F.; Utama, W.; Hamdan, A.M.; Bijaksana, S.; Pratama, A.; Yunginger, R.; Sudarningsih, S. Heavy Metal Contents and Magnetic Properties of Surface Sediments in Volcanic and Tropical Environment from Brantas River, Jawa Timur Province, Indonesia. *Sci. Total Environ.* **2019**, *675*, 632–641. https://doi.org/10.1016/j.scitotenv.2019.04.244.
24. Guda, A.M.; El Kammar, A.M.; Abu Salem, H.S.; Abu Khatita, A.M.; Mohamed, M.A.; El-Hemaly, I.A.; Abd Elaal, E.M.; Odah, H.H.; Appel, E. Integrated Geochemical and Magnetic Potentially Toxic Elements Assessment: A Statistical Solution

Discriminating Anthropogenic and Lithogenic Magnetic Signals in a Complex Area of the Southeast Nile Delta. *Environ. Monit. Assess.* **2024**, *196*, 272. https://doi.org/10.1007/s10661-024-12408-5.

25. Yang, X.; An, N.; Luo, H.; Zheng, J.; Wu, J.; Yang, D. Phragmites Australis Elevated Concentrations of Soil-Bound Heavy Metals and Magnetic Particles in a Typical Urban Plateau Lake Wetland, China. *Heliyon* **2025**, *11*, e41528. https://doi.org/10.1016/j.heliyon.2024.e41528.
26. Su, Z.; Shen, S.; Yang, X.; Liu, Y.; Yang, H.; He, S. Unraveling the Complex Interplay between Magnetic Properties and Toxic Metals in Fluvial Sediments. *Ecotoxicol. Environ. Saf.* **2025**, *303*, 118825. https://doi.org/10.1016/j.ecoenv.2025.118825.
27. Chrysakopoulou, C.; Aidona, E.; Vogiatzis, D.; Drakoulis, A.; Papadopoulou, L.; Kantiranis, N. Environmental Profile Assessment in a Highly Industrialized Area Through Magnetic Susceptibility Spatial Variations and Morphological Study of Magnetic Particles: The Case of Sarigiol Basin (Greece). *Pollutants* **2025**, *5*, 4. https://doi.org/10.3390/pollutants5010004.
28. Buynevich, I.V.; Tõnisson, H.; Rosentau, A.; Hang, T.; Kont, A.; Tamura, T.; Suuroja, S.; Palginõmm, V.; Döring, S.F.S. Rapid Magnetic Susceptibility Characterization of Coastal Morphosedimentary Units at Two Insular Strandplains in Estonia. *J. Mar. Sci. Eng.* **2023**, *11*, 232. https://doi.org/10.3390/jmse11020232.
29. Lei, P.; Xu, X.; Yang, Z.; Wang, Q.; Hou, L.; Jin, Y.; Wu, Q. Magnetic Mineral Dissolution in Heqing Core Lacustrine Sediments and Its Paleoenvironment Significance. *Minerals* **2024**, *14*, 1096. https://doi.org/10.3390/min14111096.
30. Yang, L.; Chen, P.; Xie, Y.; Liu, S.; Chen, N.; Tian, Y.; Zhang, X.; Shang, J.; Jia, J. Magnetic ‘Fingerprinting’ of Sediments in Taizhou Bay: Implications for Provenance. *Geosciences* **2025**, *16*, 20. https://doi.org/10.3390/geosciences16010020.
31. Gomes, P.; Valente, T.; Font, E. Integrated Characterization of Sediments Contaminated by Acid Mine Drainage: Mineralogical, Magnetic, and Geochemical Properties. *Minerals* **2025**, *15*, 786. https://doi.org/10.3390/min15080786.
32. Xia, F.; Liu, D.; Zhang, Y. Characteristics and Environmental Indications of Grain Size and Magnetic Susceptibility of the Late Quaternary Sediments from the Xiyang Tidal Channel, Western South Yellow Sea. *J. Mar. Sci. Eng.* **2024**, *12*, 699. https://doi.org/10.3390/jmse12050699.
33. Wen, R.; Liang, S.; Li, M.; Chaparro, M.A.E.; Yuan, Y. Coarse and Fine-Grained Sediment Magnetic Properties from Upstream to Downstream in Jiulong River, Southeastern China and Their Environmental Implications. *J. Mar. Sci. Eng.* **2025**, *13*, 1502. https://doi.org/10.3390/jmse13081502.
34. Pađan, J.; Marcinek, S.; Cindrić, A.-M.; Layglon, N.; Garnier, C.; Salaün, P.; Cobelo-García, A.; Omanović, D. Determination of Sub-Picomolar Levels of Platinum in the Pristine Krka River Estuary (Croatia) Using Improved Voltammetric Methodology. *Environ. Chem.* **2020**, *17*, 77–84. https://doi.org/10.1071/EN19157.
35. Marcinek, S.; Santinelli, C.; Cindrić, A.-M.; Evangelista, V.; Gonnelli, M.; Layglon, N.; Mounier, S.; Lenoble, V.; Omanović, D. Dissolved Organic Matter Dynamics in the Pristine Krka River Estuary (Croatia). *Mar. Chem.* **2020**, *225*, 103848. https://doi.org/10.1016/j.marchem.2020.103848.
36. Marcinek, S.; Cindrić, A.M.; Pađan, J.; Omanović, D. Trace Metal Partitioning in the Salinity Gradient of the Highly Stratified Estuary: A Case Study in the Krka River Estuary (Croatia). *Appl. Sci.* **2022**, *12*, 5816. https://doi.org/10.3390/app12125816.
37. Cindrić, A.M.; Garnier, C.; Oursel, B.; Pižeta, I.; Omanović, D. Evidencing the Natural and Anthropogenic Processes Controlling Trace Metals Dynamic in a Highly Stratified Estuary: The Krka River Estuary (Adriatic, Croatia). *Mar. Pollut. Bull.* **2015**, *94*, 199–216. https://doi.org/10.1016/j.marpolbul.2015.02.029.
38. Elbaz-Poulichet, F.; Guan, D.M.; Martin, J.-M. Trace Metal Behaviour in a Highly Stratified Mediterranean Estuary: The Krka (Yugoslavia). *Mar. Chem.* **1991**, *32*, 211–224. https://doi.org/10.1016/0304-4203(91)90039-Y.
39. Legović, T. Exchange of Water in a Stratified Estuary with an Application to Krka (Adriatic Sea). *Mar. Chem.* **1991**, *32*, 121–135. https://doi.org/10.1016/0304-4203(91)90032-R.
40. Lechtenfeld, O.J.; Koch, B.P.; Gašparović, B.; Frka, S.; Witt, M.; Kattner, G. The Influence of Salinity on the Molecular and Optical Properties of Surface Microlayers in a Karstic Estuary. *Mar. Chem.* **2013**, *150*, 25–38. https://doi.org/10.1016/j.marchem.2013.01.006.
41. Mikac, N.; Kwokal, Z.; May, K.; Branica, M. Mercury Distribution in the Krka River Estuary (Eastern Adriatic Coast). *Mar. Chem.* **1989**, *28*, 109–126. https://doi.org/10.1016/0304-4203(89)90190-4.
42. Bilinski, H.; Kwokal, Ž.; Plavšić, M.; Wrischer, M.; Branica, M. Mercury Distribution in the Water Column of the Stratified Krka River Estuary (Croatia): Importance of Natural Organic Matter and of Strong Winds. *Water Res.* **2000**, *34*, 2001–2010, https://doi.org/10.1016/S0043-1354(99)00366-8.
43. Martinčić, D.; Kwokal, Ž.; Branica, M. Distribution of Zinc, Lead, Cadmium and Copper between Different Size Fractions of Sediments II. The Krka River Estuary and the Kornati Islands (Central Adriatic Sea). *Sci. Total Environ.* **1990**, *95*, 217–225. https://doi.org/10.1016/0048-9697(90)90066-4.

44. Hasan, O.; Smrkulj, N.; Miko, S.; Brunović, D.; Ilijanić, N.; Šparica Miko, M. Integrated Reconstruction of Late Quaternary Geomorphology and Sediment Dynamics of Prokljan Lake and Krka River Estuary, Croatia. *Remote Sens.* **2023**, *15*, 2588. https://doi.org/10.3390/rs15102588.
45. Frančišković-Bilinski, S.; Bilinski, H.; Maldini, K.; Milović, S.; Zhang, Q.; Appel, E. Chemical and Magnetic Tracing of Coal Slag Pollutants in Karstic River Sediments. *Environ. Earth Sci.* **2017**, *76*, 476. https://doi.org/10.1007/s12665-017-6792-5.
46. Frančišković, S. Detection of Coal Combustion Products in Stream Sediments by Chemical Analysis and Magnetic-Susceptibility Measurements. *Mineral. Mag.* **2008**, *72*, 43–48. https://doi.org/10.1180/minmag.2008.072.1.43.
47. Frančišković-Bilinski, S.; Peco, J.; Sakan, S.; Đorđević, D.; Inđić, D. Magnetic and Geochemical Properties of Zagreb City Area Soils. *Minerals* **2023**, *13*, 1481. https://doi.org/10.3390/min13121481.
48. Prohić, E.; Juračić, M. Heavy Metals in Sediments-Problems Concerning Determination of the Anthropogenic Influence. Study in the Krka River Estuary, Eastern Adriatic Coast, Yugoslavia. *Environ. Geol. Water Sci.* **1989**, *13*, 145–151, https://doi.org/10.1007/BF01664699.
49. Juračić, M.; Prohić, E. Mineralogy, Sources of Particulates, and Sedimentation in the Krka River Estuary, (Croatia). *Geološki Vjesn.* **1991**, *44*, 195–200.
50. Cukrov, N.; Barišić, D.; Juračić, M. Calculated Sedimentation Rate in the Krka River Estuary Using Vertical Distribution of ^{137}Cs. In Proceedings of the 38th CIESM Congress, Istanbul, Turkey, 9–13 April 2007.
51. Bogner, D.; Ujević, I.; Zvonarić, T.; Barić, A. Distribution of Selected Trace Metals in Coastal Surface Sediments from the Middle and South Adriatic. *Fresenius Environ. Bull.* **2004**, *13*, 1281–1287.
52. Cukrov, N.; Cindrić, A.M.; Omanović, D.; Cukrov, N. Spatial Distribution, Ecological Risk Assessment, and Source Identification of Metals in Sediments of the Krka River Estuary (Croatia). *Sustainability* **2024**, *16*, 1800. https://doi.org/10.3390/su16051800.
53. Cukrov, N.; Cukrov, N.; Omanović, D. Early Diagenetic Processes in the Sediments of the Krka River Estuary. *J. Mar. Sci. Eng.* **2024**, *12*, 466. https://doi.org/10.3390/jmse12030466.
54. Reimann, C.; Filzmoser, P.; Garrett, R.G. Background and Threshold: Critical Comparison of Methods of Determination. *Sci. Total Environ.* **2005**, *346*, 1–16. https://doi.org/10.1016/j.scitotenv.2004.11.023.
55. Tukey, J.W. *Exploratory Data Analysis*; Addison-Wesley: Reading, MA, USA, 1977.
56. Kaufman, L.; Rousseeuw, P.J. *Finding Groups in Data*; Wiley: Hoboken, NJ, USA, 1990.
57. Halamić, J.; Peh, Z.; Bukovec, D.; Miko, S.; Galović, L. A Factor Model of the Relationship between Stream Sediment Geochemistry and Adjacent Drainage Basin Lithology, Medvednica Mt., Croatia. *Geol. Croat.* **2001**, *54*, 37–51. https://doi.org/10.4154/GC.2001.04.
58. Davis, J.C. *Statistics and Data Analysis in Geology*; Wiley: Hoboken, NJ, USA, 2002.
59. Frančišković Bilinski, S.; Dolenec, M.; Hamarashid, R.; Mohialdeen, I.M.J.; Fiket, Ž. Magnetic Susceptibility as a Rapid Tool for Heavy Metal Pollution Assessment near Coal Ash Landfills and Metallurgical Complexes. *J. Soils Sediments* 2026, *submitted.*
60. Frančišković-Bilinski, S.; Bilinski, H.; Scholger, R.; Tomašić, N.; Maldini, K. Magnetic Spherules in Sediments of the Karstic Dobra River (Croatia). *J. Soils Sediments* **2014**, *14*, 600–614. https://doi.org/10.1007/s11368-013-0808-x.
61. Mukaka, M.M. Statistics Corner: A Guide to Appropriate Use of Correlation Coefficient in Medical Research. *Malawi Med. J.* **2012**, *24*, 69–71.
62. Ayoubi, S.; Adman, V.; Yousefifard, M. Use of Magnetic Susceptibility to Assess Metals Concentration in Soils Developed on a Range of Parent Materials. *Ecotoxicol. Environ. Saf.* **2019**, *168*, 138–145. https://doi.org/10.1016/j.ecoenv.2018.10.024.
63. Oreščanin, V.; Barišić, D.; Mikelić, L.; Lovrenčić, I.; Rubčić, M.; Rožmarić-Mačefat, M.; Lulić, S. Environmental Contamination Assessment of the Surroundings of the Ex-Šibenik's Ferro-Manganese Smelter, Croatia. *J. Environ. Sci. Health Part A* **2004**, *39*, 2493–2506. https://doi.org/10.1081/ESE-200026329.
64. Iswanto, B.H.; Zulaikah, S. Selection Method to Identify the Dominant Elements That Contribute to Magnetic Susceptibility in Sediment. *J. Phys. Conf. Ser.* **2019**, *1402*, 044087. https://doi.org/10.1088/1742-6596/1402/4/044087.
65. Zhao, X.; Zhang, J.; Ma, R.; Luo, H.; Wan, T.; Yu, D.; Hong, Y. Worldwide Examination of Magnetic Responses to Heavy Metal Pollution in Agricultural Soils. *Agriculture* **2024**, *14*, 702. https://doi.org/10.3390/agriculture14050702.
66. Karimi, A.; Haghnia, G.H.; Ayoubi, S.; Safari, T. Impacts of Geology and Land Use on Magnetic Susceptibility and Selected Heavy Metals in Surface Soils of Mashhad Plain, Northeastern Iran. *J. Appl. Geophys.* **2017**, *138*, 127–134. https://doi.org/10.1016/j.jappgeo.2017.01.022.
67. Aubineau, J.; Antonio, P.Y.J.; El Bamiki, R.; Parat, F.; Camps, P.; Raji, O.; Jourani, E.-S.; Bodinier, J.-L.; Macouin, M.; Gilder, S.; et al. Magnetic Susceptibility Controlled by Climate-Driven Weathering Intensity. *BSGF—Earth Sci. Bull.* **2024**, *195*, 25. https://doi.org/10.1051/bsgf/2024025.

68. Abdel Aal, G.Z.; Atekwana, E.A.; Revil, A. Geophysical Signatures of Disseminated Iron Minerals: A Proxy for Understanding Subsurface Biophysicochemical Processes. *J. Geophys. Res. Biogeosciences* **2014**, *119*, 1831–1849. https://doi.org/10.1002/2014JG002659.
69. Chaparro, M.A.E.; Ramírez-Ramírez, M.; Chaparro, M.A.E.; Miranda-Avilés, R.; Puy-Alquiza, M.J.; Böhnel, H.N.; Zanor, G.A. Magnetic Parameters as Proxies for Anthropogenic Pollution in Water Reservoir Sediments from Mexico: An Interdisciplinary Approach. *Sci. Total Environ.* **2020**, *700*, 134343. https://doi.org/10.1016/j.scitotenv.2019.134343.
70. Ismael, O. The Standard Deviation Score: A Novel Similarity Metric for Data Analysis. *J. Big Data* **2025**, *12*, 58. https://doi.org/10.1186/s40537-025-01091-z.